Nuclear Engineering and Technology xxx (xxxx) xxx

Contents lists available at ScienceDirect

Nuclear Engineering and Technology

journal homepage: www.elsevier.com/locate/net

Original Article

Design of Comprehensive Mechanical Properties by machine learning and high-throughput optimization algorithm in RAFM steels

Chenchong Wang [a], Chunguang Shen [a], Xiaojie Huo [b], Chi Zhang [b, *], Wei Xu [a, **]

[a] State Key Laboratory of Rolling and Automation, School of Materials Science and Engineering, Northeastern University, Shenyang 110819, China
[b] Key Laboratory of Advanced Materials of Ministry of Education, School of Materials Science and Engineering, Tsinghua University, Beijing 100084, China

ARTICLE INFO

Article history:
Received 11 August 2019
Received in revised form
13 October 2019
Accepted 21 October 2019
Available online xxx

Keywords:
Machine learning
High-throughput optimization
Mechanical property
RAFM steel

ABSTRACT

In order to make reasonable design for the improvement of comprehensive mechanical properties of RAFM steels, the design system with both machine learning and high-throughput optimization algorithm was established. As the basis of the design system, a dataset of RAFM steels was compiled from previous literatures. Then, feature engineering guided random forests regressors were trained by the dataset and NSGA II algorithm were used for the selection of the optimal solutions from the large-scale solution set with nine composition features and two treatment processing features. The selected optimal solutions by this design system showed prospective mechanical properties, which was also consistent with the physical metallurgy theory. This efficiency design mode could give the enlightenment for the design of other metal structural materials with the requirement of multi-properties.

1. Introduction

Since materials genome initiative (MGI) was put forward with the intent 'to discover, manufacture, and deploy advanced materials twice as fast, at a fraction of the cost', the materials design by integrated computing became one of the hot topics in the field of special steels [1–3]. In order to partially avoid large amount of orthogonal experiments, various computing strategies, as multi-scale models based on physical metallurgy principles [4,5], machine learning (ML) methods [6,7], optimization algorithms [8,9], etc., were used to guide the modification of the composition or treatment process of steels.

As one of the most well-known examples, G.B. Olson's group from northwestern university developed two forms of steel (Ferrium S53 and Ferrium M54), which were licensed to QuesTek Innovation, LLC. Ferrium S53 was used in landing gears for the U.S. air force and Ferrium M54 was used on the safety-critical hook shank component [1,10]. During the development of Ferrium S53 and Ferrium M54, multi-scale models based on physical metallurgy principles were used and successfully guided the improvement of the comprehensive mechanical properties, as the strength, fracture toughness and hydrogen embrittlement resistance ability. However, the accuracy of physical metallurgy models critically depended on the clear physical mechanism and accurate thermodynamic database, which limited their scope of application. Therefore, in order to avoid the limitation of physical mechanism, several recent researches focused on the ML algorithm. Various different ML models, as support vector machine (SVM) [11,12], artificial neural network (ANN) [13,14], random forests regressors (RFR) [15], etc. were used for the prediction of various properties. Recently, S.F. Long et al. [16] established a ML model for the prediction of tensile properties by GDM-SA-SVR algorithm for RAFM steels. This model could provide a relatively accurate prediction of RAFM steels' yield strength with the effect of both irradiation and high temperature. Also, for the irradiation swelling, M.M. Jin et al. [17] made a systematically discussion about the prediction of void swelling in different steels by ML algorithm. In their research, different ML algorithms were compared to analyze the optimal strategy for the prediction. However, most researches based on ML algorithm in the field of steels design only focused on one objective without the comprehensive consideration of different properties. Also, with the limitation of data amount for different steels, the improvement of generalization ability was a common problem in most researches based on ML algorithms. For the design of reduced activation ferritic/martensitic (RAFM) steels, Lu et al. [18] used CALPHAD theory combined with optimization algorithm to design both the solidification and dispersion strengthening. And the designed

* Corresponding author.
** Corresponding author.
E-mail addresses: chizhang@tsinghua.edu.cn (C. Zhang), xuwei@ral.neu.edu.cn (W. Xu).

https://doi.org/10.1016/j.net.2019.10.014

results were used to guide the improvement of creep of RAFM steels. However, the design by Lu was also focused on only one objective (creep) without considering the comprehensive design of multi-property.

In summary, most previous researches used physical metallurgy models were limited by the controversial physical mechanism. And most design of RAFM steels was mainly focused on one special properties. In this work, in order to overcome the complex physical mechanism of mechanical properties, especially impact toughness, ML models were established to predict the comprehensive mechanical properties of RAFM steels. Then, a high-throughput multi-objective optimization algorithm was used to make a comprehensive design of RAFM steels. This design mode could also give the enlightenment for the design of other metal structural materials.

2. Simulation method

2.1. Property prediction method by ML algorithm

In order to obtain relatively accurate models for the prediction of comprehensive mechanical properties of RAFM steels, ML was used and models were trained by the dataset established from Refs. [19–29] as shown in Fig. 1(a). The dataset of RAFM steels contained 60 groups of data about RAFM steels, including traditional RAFM steels from different countries and new designed alloys by different institutes. The information of every group of data included 11 critical input features (content of C, Cr, W, Si, V, Ta, Ti, N, B, tempering temperature and time) and 2 outputs (YS: yield strength; IT: impact toughness) as shown in Table 1. Then, in order to further enhance the generalization ability of ML models, standard feature engineering process was used to obtain the seven highest correlated features for the training of the ML models for different properties. The RF algorithm was used to assess the importance of the 11 features quantitatively by comparing the variation of predicted accuracy of OOB (out of bag) samples for selected features with/without random noise, and then "last-place elimination" rules were used to efficiently exclude the features which had less effect on the property prediction. Also, standard normalization processing was used as the preprocessing method to reduce dimensional differences between different inputs and outputs. Then, after the partitioning of the dataset, the RAFM dataset was divided into a training dataset with 80% groups of data (48 groups) and a test dataset with 20% groups of data (12 groups). Finally, feature engineering guided random forests regressors (FE-RFRs) were trained for the prediction of both yield strength and impact toughness of RAFM steels.

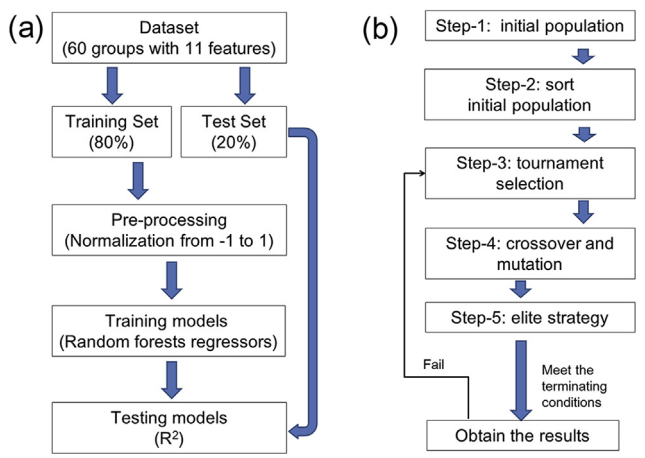

Fig. 1. Framework of the design system: (a) ML algorithm; (b) high-throughput optimization algorithm.

Table 1
Value of the inputs and outputs from the dataset of RAFM steels.

	Features' name	Value of the features			Standard deviation
		Max	Min	Mean	
Inputs	C (wt.%)	0.13	0.03	0.10	0.02
	Cr (wt.%)	9.30	4.61	7.71	1.74
	W (wt.%)	3.01	0.00	1.84	0.70
	Si (wt.%)	0.77	0.00	0.16	0.11
	V (wt.%)	0.30	0.05	0.23	0.04
	Ta (wt.%)	0.55	0.00	0.08	0.08
	Ti (wt.%)	0.15	0.00	0.01	0.04
	N (wt.%)	0.43	0.00	0.02	0.06
	B (wt.%)	0.01	0.00	0.001	0.003
	Temp (°C)	780.00	650.00	737.87	27.88
	Time (min)	120.00	30.00	74.00	29.23
Outputs	YS (MPa)	824.00	464.00	621.44	99.57
	IT (J)	342.50	16.25	170.90	81.29

2.2. Design method by high-throughput optimization algorithm

For the design process, the 2nd generation of non-dominated sorting genetic algorithms (NSGA II) [30–33], which combined traditional NSGA with elitist strategy, was used for the two objective high-throughput optimization (both yield strength and impact toughness). The process of NSGA II was shown in Fig. 1(b). Firstly, the first generation set with 200 solutions containing all the correlated features was randomly created. The information storage chain of the solutions with all the value of features was defined as the 'chromosomes' of the solutions. Then the objective value (yield strength and impact toughness) was calculated by FE-RFRs for all the 200 solutions in the first generation set. Also, the crowding degree for all the 200 solutions was evaluated by the Euler distance to the closest solution. By evaluating and sorting based on the objective value and crowding degree, the Pareto front for the 1st generation set could be obtained. Then, a genetic operator was utilized to produce offsprings from parent chromosomes. Based on the calculated results of Pareto front, the genetic operators made crossover and mutation for the information storage chain of solutions in 1st generation set to create new solutions. Finally, elitist strategy was used to select the optimal solutions to form the 2nd generation set. By this kind of cyclic iteration, the solutions would be efficiently optimized with the evolution of the generation.

3. Results and discussion

3.1. Prediction results

The prediction results of both yield strength and impact toughness were shown in Fig. 2(a) and (b). For the yield strength prediction, the squared correlation coefficient (R^2) between experimental value and predicted value was larger than 90% for both training and test sets (92.7% for training set and 91.1% for test set). Also, similar results of R^2 were obtained for impact toughness prediction (92.3% for training set and 85.6% for test set). It meant that all the FE-RFRs trained in this research had relatively high generalization ability and suitable for the prediction of traditional mechanical properties in the field of RAFM steels. Also, Fig. 2(a) showed that the mean absolute deviation (MAE) of the predicted yield strength was less than 26 MPa, which was significant lower than previous researches (MAE = 50 MPa) [34], which used multi-scale phenomenological models based on the theory of physical metallurgy to predict the yield strength. Also, for the impact

Please cite this article as: C. Wang et al., Design of Comprehensive Mechanical Properties by machine learning and high-throughput optimization algorithm in RAFM steels, Nuclear Engineering and Technology, https://doi.org/10.1016/j.net.2019.10.014

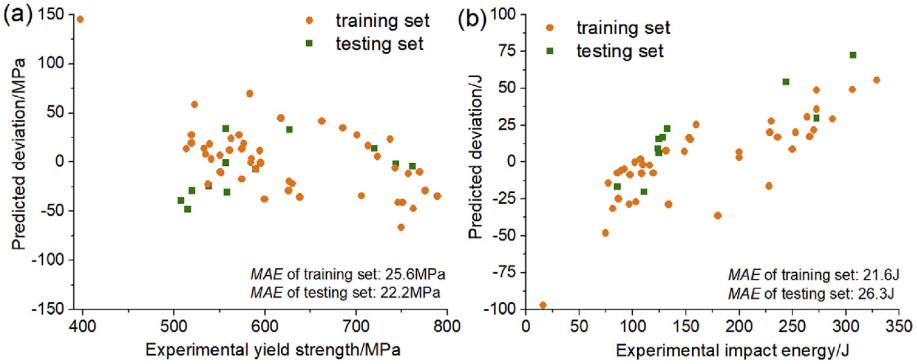

Fig. 2. Prediction results by FE-RFRs: (a) MAE of the yield strength; (b) MAE of the impact toughness.

toughness, which was hardly predicted by physical metallurgy models, MAE was less than 27 J. These results indicated that FE-RFRs could obtain better accuracy and universality than previous multi-scale physical metallurgy models for the prediction of comprehensive mechanical properties in the field of RAFM steels.

3.2. Design results

Fig. 3 showed the designed results with the predicted yield strength and impact toughness of the optimal solutions found by NSGA II. The optimal solutions were obtained from the last generation after 10^5 cyclic iterative calculating by NSGA II. It could be seen that the optimal solutions formed the obvious Pareto front, which represented the comprehensive optimization of both yield strength and impact toughness. Also, the mechanical properties for traditional RAFM steels (Eurofer97, CLAM and CLF), which were reported by previous researches, were shown in Fig. 3. It was significant that the predicted results of most optimal solutions were relatively higher than traditional RAFM steels. The highest predicted yield strength of the optimal solutions could reach 800 MPa, which was more than 120 MPa higher than traditional RAFM steels. Also, at the same time, it could maintain acceptable impact toughness (150 J), which could meet the requirement of China fusion engineering testing reactor (CFETR) [35,36]. Table 2 showed the designed composition and treatment parameters of five selected optimal solutions. Most design results of the selected optimal solutions showed relatively high yield strength (>700 MPa) and improved impact toughness (>200 J). Also, it was worth to be mentioned that, as well-known, it was difficult to prove that the final generation obtained by GA was the ideal optimal solution for the whole searching area. Therefore, the 'optimal solutions' shown in Table 2 was only the improved solutions obtained by 10^5 cyclic iterative.

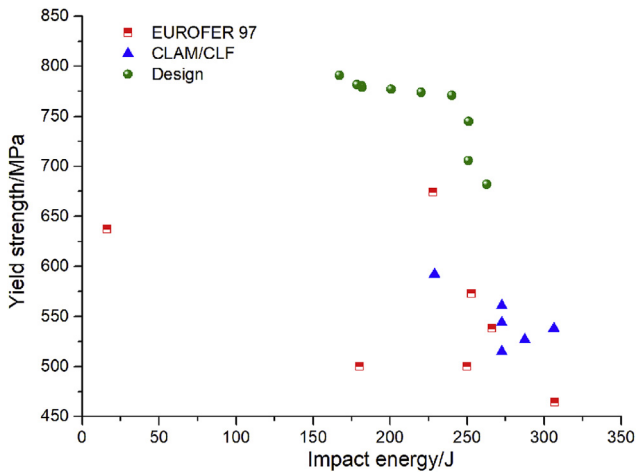

Fig. 3. Comparison of the designed results and traditional RAFM steels.

Also, Fig. 4 showed the comparison results of the composition between the selected optimal solutions and Eurofer97 (Fe-0.1C–9Cr–1W-0.2V-0.1Ta). In order to eliminate dimensional differences between different elements, the percentages of the changes for original elements (C, Cr, W, V, Ta) were used to estimate the modification of the composition. For the original elements, most designed solutions maintained the basic composition system of Fe-0.1C–9Cr–2W, which was commonly used in traditional heat-resistant steels [21]. For Eurofer97, the content of W decreased to 1.3 wt% in order to inhibit the formation of laves phases. However, in most designed solutions, instead of deceasing the content of W, 0.16 wt% Si was added to inhibit the adverse effect of laves phases. Also, Ti was used to partly replace the function of V for precipitation strengthening, because TiC had stronger stability than VC during the service condition with relatively high temperature (>650 °C). In summary, based on the experience of physical metallurgy, it was indicated that the designed solutions had reasonable composition and could probably obtain better mechanical properties than traditional RAFM steels and they should be worth for experimental verification.

3.3. Expanding ability of the design system

In order to compare the optimal solutions and the original alloys in the dataset, Spearman correlation coefficient is applied to calculate their similarity. Fig. 5 showed the difference between the selected optimal solutions and the original alloys in the dataset with the highest yield strength/impact toughness. It could be seen that the composition and treatment parameters of the selected optimal solutions were different with the original alloys from the dataset. Especially for the designed solution of 1# and 2#, the degree of correlation between designed solution of 1#/2# and the original alloys with the highest yield strength/impact toughness was all less than 0.9. It indicated that this design system had acceptable expanding ability and it could help to find innovative alloys for the improvement of comprehensive mechanical properties.

However, the FE-RFRs trained in this research also had its scope of application. In the range of 0.03–0.13 wt %C, 4.61–9.30 wt % Cr, 0–3.01 wt % W, 0–0.77 wt % Si, 0.05–0.3 wt % V, 0–0.55 wt % Ta, 0–0.15 wt % Ti, tempering temperature 650–780 °C, tempering time 30–120 min, the prediction error of the models could probably be <10% for both yield strength and impact toughness.

Please cite this article as: C. Wang et al., Design of Comprehensive Mechanical Properties by machine learning and high-throughput optimization algorithm in RAFM steels, Nuclear Engineering and Technology, https://doi.org/10.1016/j.net.2019.10.014

Table 2
Designed composition and treatment parameters for the selected optimal solutions.

No.	Composition (wt. %)									TT (°C)	Tt (min)	YS (MPa)	IM (J)
	C	Cr	W	Si	V	Ta	Ti	N	B				
1#	0.11	8.7	2.0	0.20	0.05	0.19	0.01	0.02	0.001	688	70	791	168
2#	0.10	8.6	1.9	0.16	0.06	0.10	0.05	0.005	0.002	714	80	682	263
3#	0.11	8.7	1.9	0.16	0.13	0.11	0.02	0.02	0.001	710	69	780	182
4#	0.10	8.7	2.0	0.16	0.13	0.10	0.02	0.01	0.001	711	45	771	240
5#	0.10	8.7	1.8	0.16	0.06	0.10	0.13	0.01	0.001	662	52	745	251

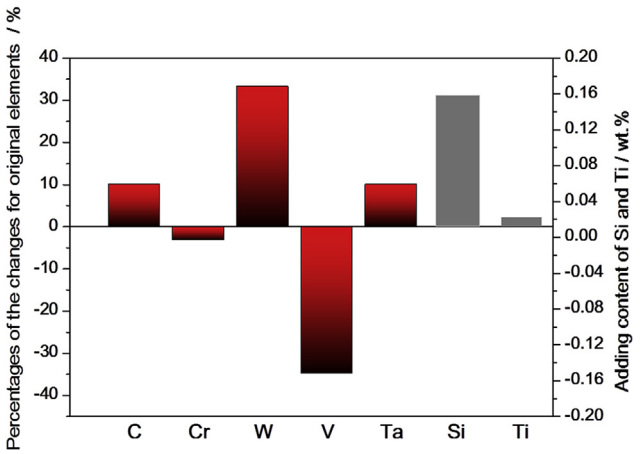

Fig. 4. Comparison results of the composition between the selected optimal solutions and Eurofer97.

However, when beyond this range occurred, the prediction error of the models was hard to estimate. Therefore, further improvement should also be made for broadening the application scope of these models. This is also one of the hot topics in the field of materials design by ML. Also, several ideas were proposed for improving the expanding ability of ML models, as adding thermodynamic features [37], introducing physical metallurgy constraints [38], etc. The main disadvantage of physical metallurgy model was that some ideal assumptions used in the models were not accurately consistent with the reality, which would limit the performance of the model. However, the introduce of physical metallurgy constraints to ML models could help to expand the application scope and improve the rationality and explicability of ML models. Therefore, the combination of physical metallurgy models and ML models was a bright way for the development of ML for alloy design. In addition to combining ML model with selected physical features, some improved model evaluation methods have been proposed for measuring the expanding ability of ML model. In work of Xiong et al. [39], they proposed a family of *k*-fold-*m*-step forward cross-validation methods as a new evaluation approach for ML model for explorative prediction, and results displayed that proposed method can more accurately evaluate the performance of the ML model than traditional CV approach.

4. Conclusion

A design system based on ML and high-throughput optimization algorithm was established to obtain the optimal solutions of RAFM steels with both composition and treatment process modification for the improvement of both yield strength and impact toughness. For the part of ML, the trained FE-RFRs had acceptable generalization ability (R^2>85%) and could obtain better accuracy and universality than previous multi-scale physical metallurgy models. For the part of high-throughput optimization, five selected optimal solutions were finally obtained by NSGA II algorithm. Most selected optimal solutions showed relatively high yield strength (>700 MPa) and improved impact toughness (>200 J) and should be worth for experimental verification. This design mode could help to obtain innovative RAFM steels with improved comprehensive mechanical properties and give the enlightenment for the design of other metal structural materials.

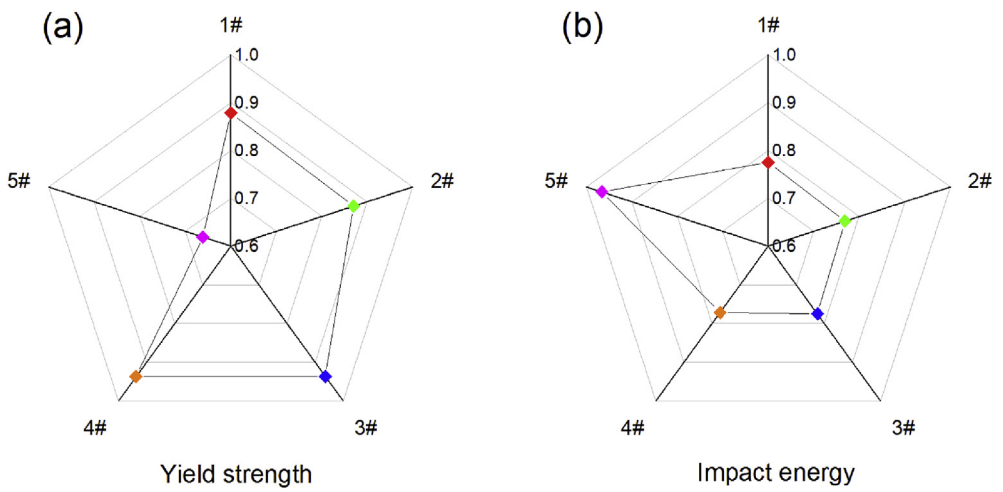

Fig. 5. Calculation results of the correlation degree: (a) for the original alloy with the highest yield strength; (b) for the original alloy with the highest impact toughness.

Please cite this article as: C. Wang et al., Design of Comprehensive Mechanical Properties by machine learning and high-throughput optimization algorithm in RAFM steels, Nuclear Engineering and Technology, https://doi.org/10.1016/j.net.2019.10.014

Declaration of competing interest

The authors declared that we have no conflicts of interest to this work (NETJOURNAL_2019_592: Design of Comprehensive Mechanical Properties by Machine Learning and High-throughput Optimization Algorithm in RAFM Steels).

We declare that we do not have any commercial or associative interest that represents a conflict of interest in connection with the work submitted.

Acknowledgements

This work was financially supported by National Natural Science Foundation of China (Grant No. 51801019 and Grant No. 51574080). Greatly acknowledged the financial support provided by Basic Scientific Research Funds of Northeastern University (N170703004).

Appendix A. Supplementary data

Supplementary data to this article can be found online at https://doi.org/10.1016/j.net.2019.10.014.

References

[1] G.B. Olson, Genomic materials design: the ferrous frontier, Acta Mater. 61 (2013) 771–781.
[2] C. Wang, C. Zhang, Z. Yang, J. Su, Y. Weng, Multi-scale simulation of hydrogen influenced critical stress intensity in high Co–Ni secondary hardening steel, Mater. Des. 87 (2015) 501–506.
[3] C. Wang, C. Zhang, Z. Yang, J. Su, Y. Weng, Microstructure analysis and yield strength simulation in high Co–Ni secondary hardening steel, Mater. Sci. Eng. A 669 (2016) 312–317.
[4] C. Wang, C. Zhang, Z. Yang, J. Zhao, Multiscale simulation of yield strength in reduced-activation ferritic/martensitic steel, Nucl. Eng. Technol. 49 (2017) 569–575.
[5] J.S. Wang, M.D. Mulholland, G.B. Olson, D.N. Seidman, Prediction of the yield strength of a secondary-hardening steel, Acta Mater. 61 (2013) 4939–4952.
[6] S. Datta, F. Pettersson, S. Ganguly, H. Saxén, N. Chakraborti, Designing High strength multi-phase steel for improved strength–ductility balance using neural networks and multi-objective genetic algorithms, ISIJ Int. 47 (2007) 1195–1203.
[7] S. Datta, F. Pettersson, S. Ganguly, H. Saxén, N. Chakraborti, Identification of factors governing mechanical properties of TRIP-aided steel using genetic algorithms and neural networks, Mater. Manuf. Process. 23 (2008) 130–137.
[8] S. Ganguly, S. Datta, N. Chakraborti, Genetic algorithms in optimization of strength and ductility of low-carbon steels, Mater. Manuf. Process. 22 (2007) 650–658.
[9] S. Ganguly, S. Datta, N. Chakraborti, Genetic algorithm-based search on the role of variables in the work hardening process of multiphase steels, Comput. Mater. Sci. 45 (2009) 158–166.
[10] C. Wang, C. Zhang, Z. Yang, J. Su, Y. Weng, Analysis of fracture toughness in high Co–Ni secondary hardening steel using FEM, Mater. Sci. Eng. A 646 (2015) 1–7.
[11] A. Bernieri, G. Betta, L. Ferrigno, M. Laracca, S. Mastrostefano, Multifrequency excitation and support vector machine regressor for ECT defect characterization, IEEE Trans. Instrum. Meas. 63 (2014) 1272–1280.
[12] Z. Han, Y. Liu, J. Zhao, W. Wang, Real time prediction for converter gas tank levels based on multi-output least square support vector regressor, Contr. Eng. Pract. 20 (2012) 1400–1409.
[13] R. Kemp, G.A. Cottrell, H.K.D.H. Bhadeshia, G.R. Odette, T. Yamamoto, H. Kishimoto, Neural-network analysis of irradiation hardening in low-activation steels, J. Nucl. Mater. 348 (2006) 311–328.
[14] F.Y. Lu, Z.Q. Yin, C. Wang, C.H. Cui, J. Teng, S. Wang, W. Chen, W. Huang, B.J. Xu, G.C. Guo, Z.F. Han, Parameter optimization and real-time calibration of a measurement-device-independent quantum key distribution network based on a back propagation artificial neural network, J. Opt. Soc. Am. B 36 (2019) B92–B98.
[15] J. Ding, Z. Bar-Joseph, MethRaFo: MeDIP-seq methylation estimate using a random forest regressor, Bioinformatics 33 (2017) 3477–3479.
[16] S.F. Long, M. Zhao, X.F. He, Yield stress prediction model of RAFM steel based on the improved GDM-SA-SVR algorithm, Comput. Mater. Continua (CMC) 58 (2019) 727–760.
[17] M.M. Jin, P.H. Cao, M.P. Short, Predicting the onset of void swelling in irradiated metals with machine learning, J. Nucl. Mater. 523 (2019) 189–197.
[18] Q. Lu, S. van der Zwaag, W. Xu, High-throughput design of low-activation, high-strength creep-resistant steels for nuclear-reactor applications, J. Nucl. Mater. 469 (2016) 217–222.
[19] S. Chen, L. Rong, Effect of silicon on the microstructure and mechanical properties of reduced activation ferritic/martensitic steel, J. Nucl. Mater. 459 (2015) 13–19.
[20] P. Fernandez, A.M. Lancha, J. Lapena, M. Hernandez-Mayoral, Metallurgical characterization of the reduced activation ferritic/martensitic steel Eurofer'97 on as-received condition, Fusion Eng. Des. 58–59 (2001) 787–792.
[21] R.L. Klueh, D.J. Alexander, M.A. Sokolov, Effect of chromium, tungsten, tantalum, and boron on mechanical properties of 5-9Cr-WVTaB steels, J. Nucl. Mater. 304 (2002) 139–152.
[22] R.L. Klueh, J.J. Kai, D.J. Alexander, Microstructure mechanical-properties correlation of irradiated conventional and reduced-activation martensitic steels, J. Nucl. Mater. 225 (1995) 175–186.
[23] C.H. Lee, J.Y. Park, W.K. Seol, J. Moon, T.H. Lee, N.H. Kang, H.C. Kim, Microstructure and tensile and charpy impact properties of reduced activation ferritic–martensitic steel with Ti, Fusion Eng. Des. 124 (2017) 953–957.
[24] R. Ma, Y. Yang, Q. Yan, Y. Yang, X. Li, C. Ge, Effect of alloying on the properties of 9Cr low activation martensitic steels, Acta Metall. Sin. 23 (2010) 451–460.
[25] M.G. Park, C.H. Lee, J. Moon, J.Y. Park, T.H. Lee, N. Kang, H.C. Kim, Effect of microstructural evolution by isothermal aging on the mechanical properties of 9Cr-1WVTa reduced activation ferritic/martensitic steels, J. Nucl. Mater. 485 (2017) 15–22.
[26] A. Puype, L. Malerba, N. De Wispelaere, R. Petrov, J. Sietsma, Effect of W and N on mechanical properties of reduced activation ferritic/martensitic EUROFER-based steel grades, J. Nucl. Mater. 502 (2018) 282–288.
[27] L. Tan, L.L. Snead, Y. Katoh, Development of new generation reduced activation ferritic-martensitic steels for advanced fusion reactors, J. Nucl. Mater. 478 (2016) 42–49.
[28] J. Vanaja, K. Laha, M. Nandagopal, S. Sam, M.D. Mathew, T. Jayakumar, E. Rajendra Kumar, Effect of tungsten on tensile properties and flow behaviour of RAFM steel, J. Nucl. Mater. 433 (2013) 412–418.
[29] P. Wang, J. Chen, H. Fu, S. Liu, X. Li, Z. Xu, Effect of N on the precipitation behaviours of the reduced activation ferritic/martensitic steel CLF-1 after thermal ageing, J. Nucl. Mater. 442 (2013) S9–S12.
[30] H. Han, R. Yu, B. Li, Y. Zhang, Multi-objective optimization of corrugated tube inserted with multi-channel twisted tape using RSM and NSGA-II, Appl. Therm. Eng. 159 (2019).
[31] M.S. Mohammed, R.A. Vural, NSGA-II plus FEM based loss optimization of three-phase transformer, IEEE Trans. Ind. Electron. 66 (2019) 7417–7425.
[32] S. Peng, T. Li, J. Zhao, S. Lv, G.Z. Tan, M. Dong, H. Zhang, Towards energy and material efficient laser cladding process: modeling and optimization using a hybrid TS-GEP algorithm and the NSGA-II, J. Clean. Prod. 227 (2019) 58–69.
[33] B. Sen, S.A.I. Hussain, M. Mia, U.K. Mandal, S.P. Mondal, Selection of an ideal MQL-assisted milling condition: an NSGA-II-coupled TOPSIS approach for improving machinability of Inconel 690, Int. J. Adv. Manuf. Technol. 103 (2019) 1811–1829.
[34] C. Wang, C. Zhang, J. Zhao, Z. Yang, W. Liu, Microstructure evolution and yield strength of CLAM steel in low irradiation condition, Mater. Sci. Eng. A 682 (2017) 563–568.
[35] W. Wang, S. Liu, G. Xu, B. Zhang, Q. Huang, Effect of thermal aging on microstructure and mechanical properties of China low-activation martensitic steel at 550 degrees C, Nucl. Eng. Technol. 48 (2016) 518–524.
[36] S.N. Zhu, C. Zhang, Z.G. Yang, C.C. Wang, Hydrogen's influence on reduced activation ferritic/martensitic steels' elastic properties: density functional theory combined with experiment, Nucl. Eng. Technol. 49 (2017) 1748–1751.
[37] D. Shin, Y. Yamamoto, M.P. Brady, S. Lee, J.A. Haynes, Modern data analytics approach to predict creep of high-temperature alloys, Acta Mater. 168 (2019) 321–330.
[38] A. Panda, R. Naskar, S. Pal, Deep learning approach for segmentation of plain carbon steel microstructure images, IET Image Process. 13 (2019) 1516–1524.
[39] Z. Xiong, Y.X. Cui, Z.H. Liu, Y. Zhao, M. Hu, J.J. Hu, Evaluating explorative prediction power of machine learning algorithms for materials discovery using -fold forward cross-validation, Comput. Mater. Sci. 171 (2020), 109203.